Environmental Noise Retards Auditory Cortical Development

Edward F. Chang, *et al.*

Science **300**, 498 (2003);
DOI: 10.1126/science.1082163

indicating that the dynamics of the small fly are dominated by body inertia and not friction.

This assertion was further tested in several ways. First, we calculated I and C on the basis of the animal's body morphology (*6*). The values ($I = 5.2 \times 10^{-13}$ N m s^2, $C = 5.2 \times 10^{-13}$ N m s) yield a time constant $\tau = I/C = 1$ s, about 20 times the duration of a single saccade. Second, we replayed the measured wing kinematics during the saccades through the robot to generate a time course of yaw torque, T_ϕ, throughout the maneuver. We then derived I and C from a multilinear regression of T_ϕ on the measured body kinematics (*6*). This procedure yielded a value of $5.9 \times 10^{-13} \pm 3.3 \times 10^{-14}$ N m s^2 for I, and a value of $1.1 \times 10^{-12} \pm 2.3 \times 10^{-11}$ N m s for C (mean $\pm$ SD, $N = 6$). The corresponding time constant, 0.53 s, although smaller than that derived from body morphology, is still 10 times the duration of a saccade. Finally, we calculated the torque required to generate the observed body kinematics according to Eq. 1, using the morphologically based values of I and C. Given the assumptions and potential sources of error in our analysis, the time course of the predicted torque based solely on body motion and morphology matches well the time course of torque measured independently by playing the wing kinematics through the robot (Fig. 3D). It is not surprising that the torque estimated from body kinematics underestimates that measured from wing motion. The calculated value of C is most likely an overestimate because it is based on Stokes' Law and assumes a very low Reynolds number for the rotation, whereas the calculation of I is likely an underestimate because added mass effects have been ignored. Collectively, the results strongly contradict previous assumptions that the flight dynamics of flies are dominated by friction (*4, 5*).

To determine how flies change wing motion to generate yaw torque, we sorted all stroke cycles within the entire data set according to the magnitude of yaw torque created during each cycle (Fig. 3E). Two specific changes in wing motion correlate most strongly with measured yaw torque: a backward tilt of the stroke plane and an increase in stroke amplitude (Fig. 3, E and F). The backward tilt of the stroke plane accompanies an increase in the aerodynamic angle of attack that elevates flight force during the upstroke. This augmentation at the start of the upstroke has a particularly potent effect on yaw torque because the force created by the wing is roughly orthogonal to the fly's yaw axis at this point in the cycle (Fig. 3, A, B, and G). The change in torque is further augmented by an increase in stroke amplitude, which elevates wing velocity (Fig. 3G). Other parameters, such as subtle changes in angle of attack relative to the stroke path (Fig. 2B), may also play a role. At the onset of a saccade, the outside wing tilts back and beats with a greater stroke amplitude relative to the inside wing (Fig. 3F). After 12.5 ms, the conditions reverse, in accordance with the need to generate countertorque to decelerate.

These experiments show how tiny insects control aerodynamic forces to actively maneuver through their environment. Although the analyses rely on several simplifying assumptions (*6*), these are not critical for the main conclusions drawn. The internal consistency of the data further corroborates that the measurements were performed with adequate precision. The results indicate that even in small insects the torques created by the wings act primarily to overcome inertia, not friction. Because of the minor importance of frictional coupling, a countertorque is necessary to terminate the rotation of the body. The torques required to turn are produced by remarkably subtle changes in wing motion. A slight tilt of the stroke plane angle and a minor change in stroke amplitude are sufficient to accelerate the animal around the yaw axis. Although these experiments were performed on tiny fruit flies, the results are relevant for nearly all insects, because the relative importance of rotational inertia over friction increases with size. Collectively, these results provide an important basis for future research on the neural and mechanical basis of insect flight, as well as insights for the design of biomimetic flying devices.

References and Notes

1. T. S. Collett, M. F. Land, *J. Comp. Physiol.* **99**, 1 (1975).
2. C. Schilstra, J. H. van Hateren, *J. Exp. Biol.* **202**, 1481 (1999).
3. L. F. Tammero, M. H. Dickinson, *J. Exp. Biol.* **205**, 327 (2002).
4. W. Reichardt, *Naturwissenschaften* **60**, 122 (1973).
5. _____, T. Poggio, *Q. Rev. Biophys.* **9**, 311 (1976).
6. See supporting data on *Science* Online.
7. H. Wagner, *Philos. Trans. R. Soc. London Ser. B* **312**, 527 (1986).
8. C. Schilstra, J. H. van Hateren, *Nature* **395**, 654 (1998).
9. S. Vogel, *J. Exp. Biol.* **44**, 567 (1966).
10. K. G. Götz, *Kybernetik* **4**, 199 (1968).
11. C. T. David, *Physiol. Entomol.* **3**, 191 (1978).
12. S. P. Sane, M. H. Dickinson, *J. Exp. Biol.* **204**, 2607 (2001).

13. We thank J. Birch, W. Dickson, S. P. Sane, and J. Staunton for technical advice and assistance. S.N.F. thanks D. Robert for scientific advice and I. Fry-Berg for personal support. Supported by grants from NSF and the Packard Foundation (M.H.D.) and by the Swiss National Science Foundation (S.N.F.).

Supporting Online Material

www.sciencemag.org/cgi/content/full/300/5618/495/DC1
Materials and Methods
References
Movie S1

27 December 2002; accepted 21 March 2003

Environmental Noise Retards Auditory Cortical Development

Edward F. Chang* and Michael M. Merzenich

The mammalian auditory cortex normally undergoes rapid and progressive functional maturation. Here we show that rearing infant rat pups in continuous, moderate-level noise delayed the emergence of adultlike topographic representational order and the refinement of response selectivity in the primary auditory cortex (A1) long beyond normal developmental benchmarks. When those noise-reared adult rats were subsequently exposed to a pulsed pure-tone stimulus, A1 rapidly reorganized, demonstrating that exposure-driven plasticity characteristic of the critical period was still ongoing. These results demonstrate that A1 organization is shaped by a young animal's exposure to salient, structured acoustic inputs—and implicate noise as a risk factor for abnormal child development.

Soon after the onset of hearing in the rat (postnatal day 12, or P12), a large auditory cortical area dominated by broadly tuned, high-frequency–selective neurons can be defined in the temporal cortex (*1*). Through a subsequent ~2- to 3-week critical period, the infant rat's auditory cortex undergoes extensive refinement to acquire an adultlike organization. Adult rats exhibit a compact, tonotopically ordered "primary auditory cortex" (A1) that represents the full spectrum of acoustic inputs with sound frequency–selective neural responses (*1*, *2*). A1 organization is easily distorted within this early postnatal period by exposure to specific acoustic inputs, indicating that the normal development of the auditory cortex is substantially influenced (and potentially strongly biased) by the structure of environmental acoustic inputs in early life (*1*, *3*). In the human infant, the emergent selective representation of the pho-

W. M. Keck Center for Integrative Neuroscience, University of California, San Francisco, CA, USA.

*To whom correspondence should be addressed. E-mail: echang@itsa.ucsf.edu

nemic structure of the infant's native language is a probable manifestation of this powerful, sound-exposure–based critical-period plasticity (*4*).

In this study, we investigated how cortical development is affected by degraded signal-to-noise conditions. Specifically, we were interested in conditions that could simulate natural environments that apply to human infant hearing (*5*) and that could simulate the many possible inherited deficits that contribute to poor signal-to-noise conditions in central auditory processes. Previous attempts at reversibly depriving animals of natural acoustic inputs have been largely unsuccessful (*6*, *7*). A simple alternative strategy used in the present experiments was the rearing of infant rats in continuous noise applied to effectively mask normal environmental sound inputs.

Litters of rat pups were reared in continuous moderate-intensity [70 dB sound pressure level (SPL)] white noise beginning at P7, i.e., well before the commencement of hearing (*8*). The auditory cortex was subsequently electrophysiologically mapped in fine detail, within 24 hours after removal from noise exposure of rats at P16, P26, P50, and P90 (n = 3 to 4 at each age). Control animals reared under standard housing conditions were mapped at the same ages.

The development of the auditory cortex has been characterized by the progressive differentiation and refinement of a posterior zone of auditory-responsive neurons, functionally identified as A1, and by the loss of tone-evoked responsiveness over a large, broadly tuned anterior region (Fig. 1, A and B). In young rats, such as those at P16, auditory receptive fields were typically tuned to high frequencies and mostly exhibited flat, plateaued tuning curves (Fig. 1, A, D, and G). Cortical areas in which these nonselective receptive fields were recorded are denoted by hatched areas in Fig. 1A and by the red tuning curves in Fig. 1G. In older control rats (at P50 and P90) (Fig. 1, B, E, and H), the frequency representation in A1 was complete and regular, with highly selective responses predominating. These changes primarily occurred during the first month of life (control data in Fig. 1, K and L) (*1*).

By contrast, young adult, continuous noise–reared (CNR) rats retained a primitively organized auditory cortex that was mark-

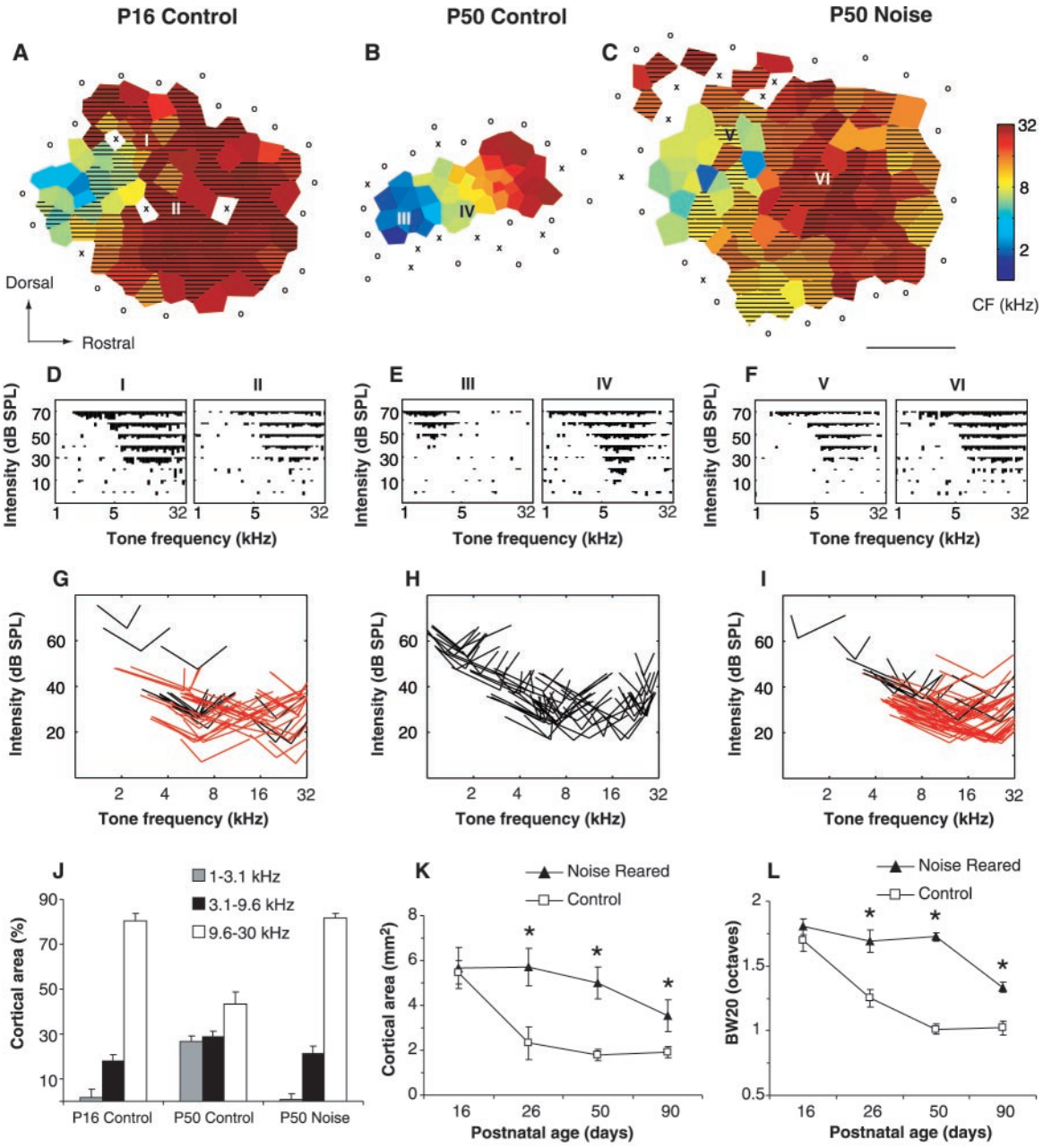

Fig. 1. Developmental organization of the auditory cortex is prolonged by noise rearing. (**A** and **B**) Representative auditory cortical characteristic frequency (CF) maps from (A) a P16 infant rat and (B) a P50 young adult rat reared in a normal acoustic environment. (**C**) Cortical map from a P50 noise-reared adult rat. Neurons sampled from the hatched areas had bandwidths at 20 dB above threshold (BW20s) that were greater than 1.5 octaves. O, unresponsive cortical site; X, non-A1 site (see text). Scale bar, 1000 μm. (**D** to **F**) Typical receptive fields recorded from the sites marked in the maps in (A) to (C). (**G** to **I**) Distribution of BW10 tuning curve tips from each map, illustrating the CF threshold, and BW10s recorded at each penetration. Red tips denote BW10s greater than 1.5 octaves. (**J**) Percentage of auditory cortex that was tuned to low, middle, or high frequencies (~1.5-octave bins). (**K**) Area of the total tone-driven cortical zone for control and CNR rats (n = 4 rats for each group). (**L**) Developmental changes in BW20 in control and CNR rats. *, $P < 0.005$. Error bars represent means ± SEM.

edly similar to that recorded in very young infant control pups (Fig. 1C). As was recorded in naïve P16 rats, adult CNR rats retained a very large tone-responsive area—on average two to three times greater than in age-matched control animals (Fig. 1, B, C, and K) (P50 control: 1.78 ± 0.28 mm^2; P50 noise-reared: 4.99 ± 0.45 mm^2; $P < 0.0001$). An immature status was also indicated by an enduring predominance of nonselective, high-frequency–tuned neurons, especially across a broad anterior auditory responsive zone in young adult CNR rats (Fig. 1, C, F, and I). The distribution of best frequencies recorded in control infant P16 pups and adult CNR rats was not significantly different, whereas both differed from those recorded in the normally reared P50 rats (Fig. 1J) [$P < 0.05$, analysis of variance (ANOVA)].

At an early developmental stage, and also in the context of noise rearing, the spectral selectivity of cortical neurons was equally poorly differentiated. Response bandwidth measures at 20 dB above threshold (BW20s, a measure of spectral selectivity) revealed that noise-reared adult animals displayed more broadly tuned neurons compared to control animals, again matching the tuning normally recorded in P16 rats (Fig. 1L) (P50 control: 1.02 ± 0.04 octaves; P50 noise-reared: 1.72 ± 0.03 octaves; $P < 0.001$). These differences in frequency representation area and spectral selectivity observed at P50 were also evident at ages P26 and P90 (Fig. 1L) ($P < 0.0001$, ANOVA across all age groups, post hoc Bonferroni corrected t test). Thus, both of these measures and others (*9*) determined at multiple benchmarks revealed a very slow, progressive organizational advance of the auditory cortex recorded in CNR rats, in sharp distinction to normally reared controls.

How do degraded acoustic conditions imposed by noise rearing alter another defining property of the developing cortex, namely, critical-period plasticity? Passive exposure of rats to pure tones during the first month of postnatal life results in the overrepresentation of those specific sounds by more selectively responding areas in A1 (*1*). As in the primary visual cortex (*10*), exposure-dependent plasticity takes place only during a limited ("critical") period, which extends from about P12 to P30 in rat A1. In post-P30 rats, cortical plasticity is contingent on behavioral context (such as attention, punishment, reward, or error monitoring), hence no substantial exposure-driven plasticity can be recorded in A1 (*11–15*).

To further test the conclusion that noise rearing delayed the end of the critical period for A1, we transferred sexually mature adult CNR rats at ages P50 and P90 to a second sound-attenuation chamber and exposed them to a 7-kHz tone train (seven repetitions in 1 s, every 5 s). After 2 weeks in this new sound environment, the auditory cortices of these rats were mapped as described previously. A1 in these tone-exposed CNR rats substantially overrepresented 7 kHz as compared with A1 in control rats (in a range of ±0.3 octaves; $n = 4$ rats per group, $P < 0.001$, ANOVA) (Fig. 2, A and B). Representations of immediately lower and higher frequencies (in 0.6-octave bins) were also sharply and selectively reduced in extent (Fig. 2, G to J) ($P < 0.005$, ANOVA). Age-matched control rats exposed to pure tones on an identical schedule did not differ from naïve controls, again confirming that a critical period, defined as an epoch of exposure-based reorganization of the auditory cortex, had ended for those animals.

CNR rats that received a 7-kHz exposure also displayed residual effects of the noise exposure. Although the overall auditory cortical area had decreased and most sampled neurons

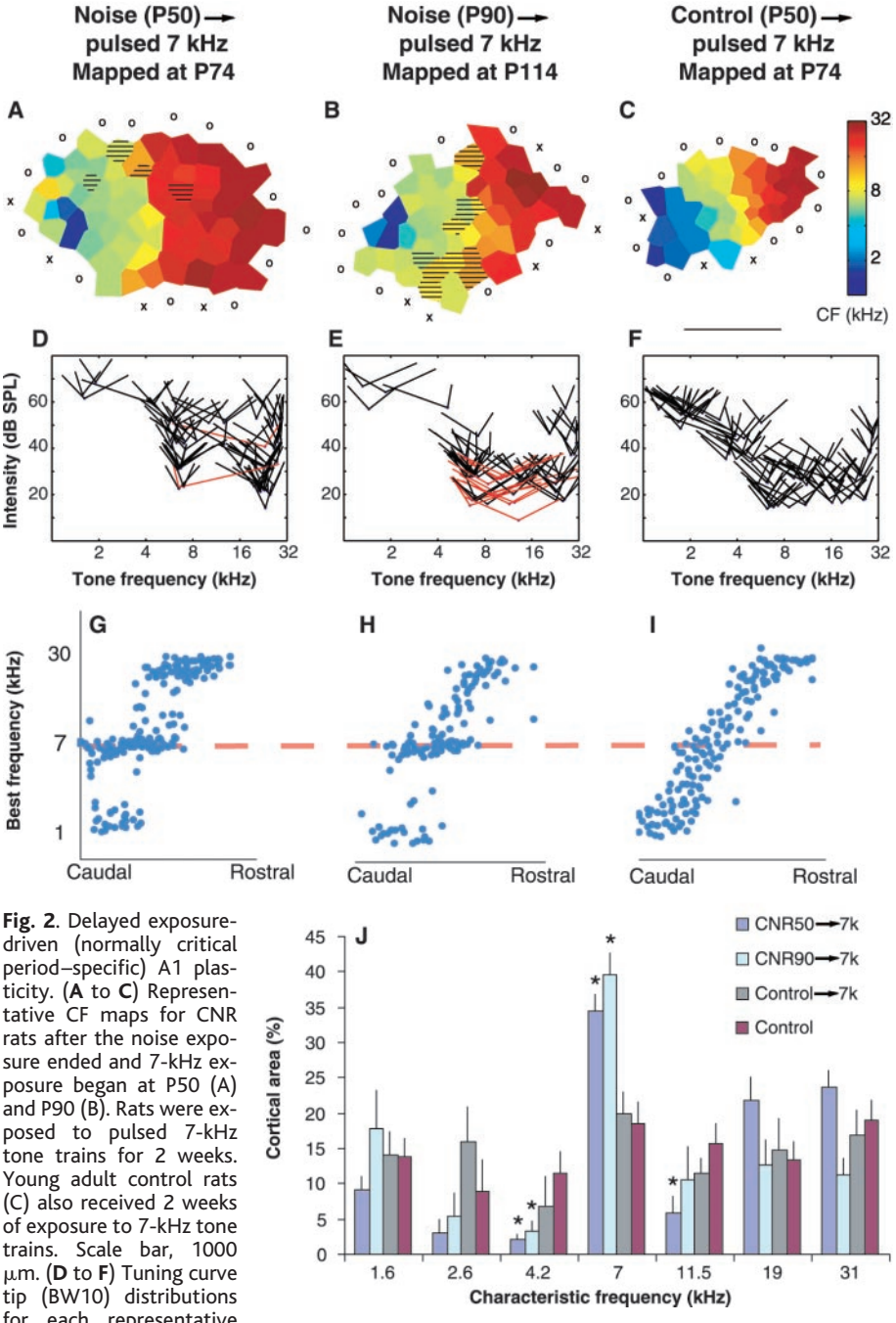

Fig. 2. Delayed exposure-driven (normally critical period–specific) A1 plasticity. (**A** to **C**) Representative CF maps for CNR rats after the noise exposure ended and 7-kHz exposure began at P50 (A) and P90 (B). Rats were exposed to pulsed 7-kHz tone trains for 2 weeks. Young adult control rats (C) also received 2 weeks of exposure to 7-kHz tone trains. Scale bar, 1000 μm. (**D** to **F**) Tuning curve tip (BW10) distributions for each representative group. (**G** to **I**) Distributions of CFs along the anterior-posterior axis of the auditory cortex. Distances were normalized to the total length of A1. (**J**) Percentage of A1 area for representations of different CF ranges in CNR and control rats ($n = 4$ rats for each group). Bin size, 0.6 octaves; *, $P < 0.005$.

were found to be far better tuned after pure-tone exposure, some sampled A1 neurons were still broadly tuned (Fig. 2, A to F), especially in rats that were reared in continuous noise up to P90. These abnormally broadly tuned neurons were mostly located at the boundary between 7-kHz-tuned and higher frequency–tuned neurons. There was also an enduring greater cortical area that represented high-frequency–tuned neurons and a smaller area that represented neurons tuned to lower frequencies than in age-matched controls.

We also examined the long-term effects of noise rearing and of noise rearing followed by tone exposure by mapping rats 10 weeks after they were returned to standard housing conditions. In general, these CNR rats mapped at P120, long after noise cessation, exhibited characteristic frequency maps and receptive field properties that were substantially like those of control adult rats (Fig. 3, A, C, and E). That suggests that exposure-based plasticity can result in relatively normal A1 maturation in a delayed critical-period epoch, as has been described to occur in V1 (*16*). There were occasionally sampled A1 neurons that were broadly tuned, but differences with control adult rats did not reach a level of statistical significance. At the same time, the plasticity induced by pulsed pure-tone exposures in adult CNR rats showed a long-lasting, specific overrepresentation of 7-kHz tuning and an underrepresentation of lower adjacent frequencies (Fig. 3, B, D, and F). These results suggest that moderate-intensity noise rearing during early development does not necessarily permanently impair auditory cortical processing into adulthood. Once the source of noise was eliminated, the critical-period window still permitted the emergence of a relatively normal A1. Exposure-driven biases in A1 function can endure long after this long-delayed critical period was again closed, just as they endure after normal early-infancy exposure-driven biasing (*1*).

Collectively, our results demonstrate that degraded acoustic inputs delay the organizational maturation of the auditory cortex. It is likely that the effects observed in the cortex can also be recorded in subcortical auditory areas. Furthermore, the processing of signals in the context of background noise differs at different auditory system levels. Background noise in the auditory nerve, for example, increases the spontaneous rate of firing and decreases the dynamic range of spike rate intensity functions (*17*). Pure-tone bursts in background noise give rise to cortical receptive fields with higher-than-normal response thresholds, but continuous noise alone fails to elevate cortical responses above spontaneous rates under quiet conditions (*18*, *19*). The overall effect of noise on the discharge pattern of individual A1 neurons is likely to be modulated across multiple convergent inputs that shape the receptive field in both the spectral and temporal domains.

Continuous-noise rearing had different impacts on developmental maturation than does rearing in the presence of pulsed noise (*15*, *20*). Although the temporal synchronization of acoustic inputs in pulsed noise produced broader-than-normal receptive fields, those very degraded receptive fields were also incomplete, patchy, and commonly double-peaked (*15*). In both naïve infant and CNR rats, by contrast, receptive fields were characteristically broad, complete, and single-peaked (Fig. 1, D and F). Pulsed noise–reared rats at later ages did not exhibit the retention of an immature, nonselective tone-responsive cortical area as recorded in naïve infant and adult CNR rats (Fig. 1, A and C). Pulsed-noise exposure appeared to accelerate the final consolidation of a distorted cortical topography (*15*). Rats exposed to pulsed noise had substantial long-term distortions of cortical receptive fields, whereas the immature response properties recorded in noise-reared rats resolved for the most part after rats were returned to normal acoustic environments. Most importantly, rats reared in pulsed noise were not susceptible to exposure-based plasticity beyond the normal end of the critical period. These differences indicate that synchronous and temporally coherent auditory inputs, such as are present in pulsed noise and that result in the maturation of dimensions of A1 functionality, are crucial for ending the critical period of development. By contrast, the highly unstructured activities evoked by continuous noise retard cortical development and indefinitely extend the critical-period window. This observation is consistent with the finding in V1 that strengthening of locally correlated activity results in the release of one or more trophic factors (such as brain-derived neurotrophic factor) that enable changes that can close the critical-period window (*21*, *22*).

Continuous-noise rearing has also been shown to affect the development of behavior and topography in other auditory-related pro-

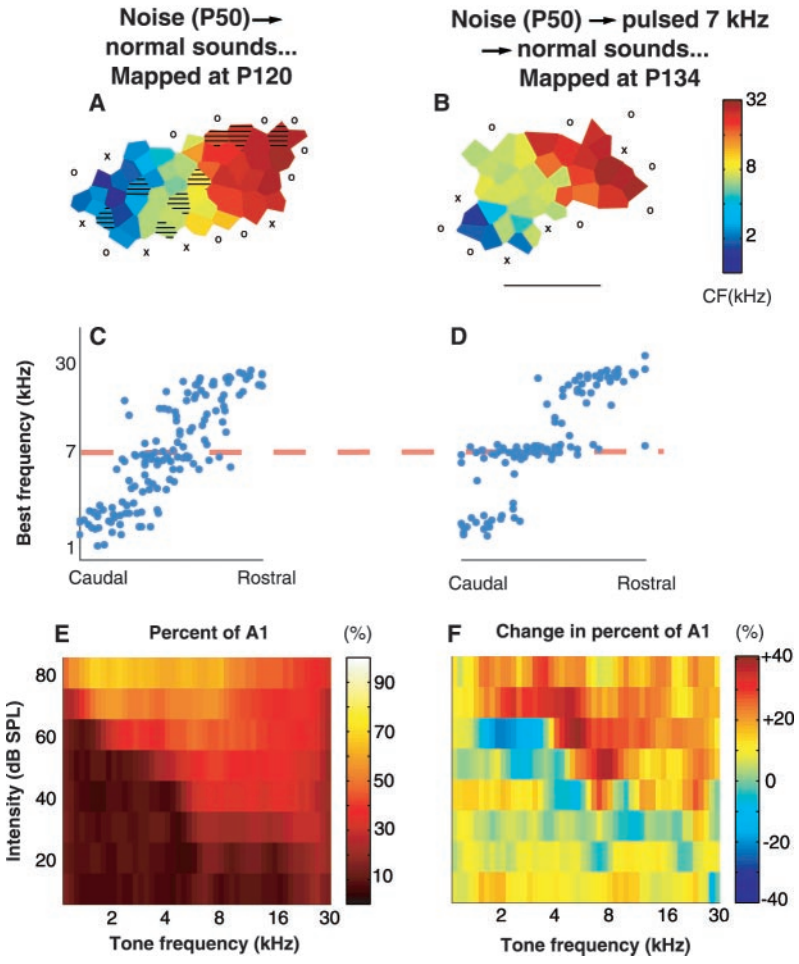

Fig. 3. Long-term effects on A1: Recovery of normal organization after a delayed critical period and persistent effects of delayed, distorting critical-period plasticity. (**A**) Representative CF map from a rat reared in continuous noise to P50, then returned to standard housing conditions for another 10 weeks. (**B**) CF map from a CNR rat exposed to 7-kHz tone trains for 2 weeks, then mapped 10 weeks later. (**C** and **D**) Distribution of CFs along the normalized tonotopic axis. (**E**) Percentage of A1 that responds to pure tones at each combination of tone frequency and intensity for recovered CNR rats (n = 4 rats). (**F**) Percentage change in A1 responses to pure tones after CNR rats were exposed to 7-kHz trains (n = 4 rats).

cesses, including vocal learning in songbirds and spatial localization in guinea pigs (*23*–*26*). The results observed here are likely due to deprivation of the instructive nature of saliently patterned spatiotemporal inputs. Similar effects are described in models of absolute sensory deprivation. In vision, for example, absolute deprivation by dark rearing similarly results in the poor maturation of orientation selectivity, less spatially selective receptive fields, degraded temporal response characteristics—and a prolongation of the critical-period plasticity as measured by the sensitivity of the primary visual cortex to the effects of monocular deprivation (*16*, *27*, *28*). In congenitally deaf cats and humans, newly introduced cochlear implants reveal poor cochleotopic organization as compared with normal hearing controls (*29*). Chronic stimulation restores many aspects of the normal activation of the auditory cortex, which is consistent with the hypothesis that severe deprivation extends the critical-period window potentially into adulthood (*29*–*31*). Our findings extend these observations of delayed cortical maturation from conditions of absolute sensory deprivation to those of signal degradation characterized by poor signal-to-noise conditions.

These studies also suggest that environmental noise, which is commonly present in contemporary child-rearing environments, can potentially contribute to auditory- and language-related developmental delays.

References and Notes

1. L. I. Zhang, S. Bao, M. M. Merzenich, *Nature Neurosci.* **4**, 1123 (2001).
2. S. L. Sally, J. B. Kelly, *J. Neurophysiol.* **59**, 1627 (1988).
3. S. G. Stanton, R. V. Harrison, *Auditory Neurosci.* **2**, 97 (1995).
4. P. K. Kuhl, K. A. Williams, F. Lacerda, K. N. Stevens, B. Lindblom, *Science* **255**, 606 (1992).
5. American Academy of Pediatrics, *Pediatrics* **100**, 724 (1997).
6. R. K. Shepherd, R. Hartmann, S. Heid, N. Hardie, R. Klinke, *Acta Otolaryngol. Suppl.* **532**, 28 (1997).
7. D. R. Moore, *Acta Otolaryngol. Suppl.* **421**, 19 (1985).
8. Materials and methods are available as supporting material on *Science* Online.
9. Other functional parameters of development, such as temporal response properties, horizontal correlation strengths, and sound intensity thresholds, are shown as supporting material on *Science* Online.
10. D. H. Hubel, T. N. Weisel, *J. Physiol. (London)* **160**, 106 (1962).
11. E. Ahissar *et al.*, *Science* **257**, 1412 (1992).
12. S. Bao, V. T. Chan, M. M. Merzenich, *Nature* **412**, 79 (2001).
13. J. M. Edeline, P. Pham, N. M. Weinberger, *Behav. Neurosci.* **107**, 539 (1993).
14. M. P. Kilgard, M. M. Merzenich, *Science* **279**, 1714 (1998).
15. L. I. Zhang, S. Bao, M. M. Merzenich, *Proc. Natl. Acad. Sci. U.S.A.* **99**, 2309 (2002).
16. M. Cynader, D. E. Mitchell, *J. Neurophysiol.* **43**, 1026 (1980).
17. J. A. Costalupes, E. D. Young, D. J. Gibson, *J. Neurophysiol.* **51**, 1326 (1984).
18. D. P. Phillips, M. S. Cynader, *Hear. Res.* **18**, 87 (1985).
19. G. Ehret, C. E. Schreiner, *Hear. Res.* **141**, 107 (2000).
20. D. H. Sanes, M. Constantine-Paton, *Science* **221**, 1183 (1983).
21. E. Castren, F. Zafra, H. Thoenen, D. Lindholm, *Proc. Natl. Acad. Sci. U.S.A.* **89**, 9444 (1992).
22. J. L. Hanover, Z. J. Huang, S. Tonegawa, M. P. Stryker, *J. Neurosci.* **19**, RC40 (1999).
23. P. Marler, M. Konishi, A. Lutjen, M. S. Waser, *Proc. Natl. Acad. Sci. U.S.A.* **70**, 1393 (1973).
24. S. Iyengar, S. W. Bottjer, *J. Neurosci.* **22**, 946 (2002).
25. D. J. Withington-Wray, K. E. Binns, S. S. Dhanjal, S. G. Brickley, M. J. Keating, *Eur. J. Neurosci.* **2**, 693 (1990).
26. M. K. Philbin, D. D. Ballweg, L. Gray, *Dev. Psychobiol.* **27**, 11 (1994).
27. G. D. Mower, D. Berry, J. L. Burchfiel, F. H. Duffy, *Brain Res.* **220**, 255 (1981).
28. L. E. White, D. M. Coppola, D. Fitzpatrick, *Nature* **411**, 1049 (2001).
29. A. Kral, R. Hartmann, J. Tillein, S. Heid, R. Klinke, *Audiol. Neurootol.* **6**, 346 (2001).
30. C. W. Ponton *et al.*, *Neuroreport* **8**, 61 (1996).
31. R. Klinke, A. Kral, S. Heid, J. Tillein, R. Hartmann, *Science* **285**, 1729 (1999).

32. We thank S. Bao for his thoughtful and informative suggestions; J. Linden, R. C. Liu, C. Atencio, K. Gobeske, and T. Moallem for technical assistance; and M. P. Stryker and L. Zhang for helpful comments. E.F.C. is a Howard Hughes Medical Institute Medical Student Research Training Fellow. Supported by NIH grants NS-10414 and NS-38416, the Coleman Fund, Hearing Research Inc., and the Mental Insight Foundation.

Supporting Online Material

www.sciencemag.org/cgi/content/full/300/5618/498/DC1
Materials and Methods
SOM Text
Figs. S1 to S3

8 January 2003; accepted 20 March 2003

Axons Guided by Insulin Receptor in *Drosophila* Visual System

Jianbo Song,[1] Lingling Wu,[1] Zun Chen,[1] Ronald A. Kohanski,[1,2] Leslie Pick[1]*

Insulin receptors are abundant in the central nervous system, but their roles remain elusive. Here we show that the insulin receptor functions in axon guidance. The *Drosophila* insulin receptor (DInR) is required for photoreceptor-cell (R-cell) axons to find their way from the retina to the brain during development of the visual system. DInR functions as a guidance receptor for the adapter protein Dock/Nck. This function is independent of Chico, the *Drosophila* insulin receptor substrate (IRS) homolog.

Insulin receptors in the central nervous system have been implicated in control of food uptake, learning, and memory, and pathophysiologies such as Alzheimer's disease (*1*–*6*). *Drosophila* harbor one receptor tyrosine kinase of the insulin receptor family (*7*–*9*), which avoids genetic redundancy in mammals that have three members of the insulin receptor family (*10*). DInR is expressed ubiquitously throughout the fly life cycle and is required for viability (*11*, *12*), longevity, and female fertility (*13*, *14*). Some combinations of hypomorphic alleles support survival, producing animals that are developmentally delayed and smaller than wild type (*11*, *12*, *15*). The growth-related phenotypes are likely mediated through Chico, a *Drosophila* IRS-like protein (*16*).

To identify additional downstream signaling partners, we used the DInR intracellular domain as bait in a yeast two-hybrid screen and identified Dreadlocks (Dock, Fig. 1A). Dock, a homolog of mammalian Nck, is an adaptor protein composed of one SH2 and three SH3 domains (*17*–*19*). Interactions between DInR and Dock depend on DInR's C-terminal tail (*11*, *20*), which contains tyrosine phosphorylation sites and proline-rich sequences and is thought to mimic some functions of insulin receptor substrates (IRSs) (*21*, *22*). A kinase-inactive form of DInR [in which Lys^{1358} is replaced by Ala (K1358A)] did not interact with Dock. DInR-K1358A was expressed at levels comparable to that of the wild type but was not detectably autophosphorylated (Fig. 1A, inset). Additional yeast two-hybrid assays indicated that DInR interacts with both the SH2 and SH3 domains of Dock (fig. S1). The absolute requirement for DInR autophosphorylation likely reflects both ligand-induced phosphotyrosine interaction(s) with Dock's SH2 domain and autophosphorylation-induced conformational change that allows the C-terminal tail to bind Dock's SH3 domains. This dual interaction is consistent with the finding that Dock's SH2 and SH3 domains can partially substitute for each other to support R-cell axon guidance (*19*).

Dock is required for R-cell axon guidance and is expressed in the neuropils of the lamina and medulla where R-cell growth cones terminate (*18*, *19*). Although we detected DInR ubiquitously, it was markedly enriched in R-cell axon projections and growth cones of third-instar larval eye-brain complexes (Fig. 1B), as is Dock (*18*, *23*), although the

[1]Brookdale Department for Molecular, Cell, and Developmental Biology, Mount Sinai School of Medicine, One Gustave Levy Place, New York, NY 10029, USA. [2]Department of Pediatrics and Department of Pharmacology and Molecular Sciences, Johns Hopkins Medical School, Baltimore, MD 21287, USA.

*To whom correspondence should be addressed. E-mail: leslie.pick@mssm.edu